Physica Medica 67 (2019) 141–147

Contents lists available at ScienceDirect

Physica Medica

journal homepage: www.elsevier.com/locate/ejmp

Original paper

Relative response of dosimeters to variations in scattered X-ray energy spectra encountered in interventional radiology

Maeve Masterson[a,*], Seán Cournane[b], Nina McWilliams[b], Dani Maguire[b], Jackie McCavana[b], Julie Lucey[b]

[a] School of Physics, National University of Ireland, Galway, Ireland
[b] Department of Medical Physics and Clinical Engineering, St Vincent's University Hospital, Dublin 4, Ireland

ARTICLE INFO

Keywords:
Eye dosimetry
Energy spectra
Interventional radiology

ABSTRACT

Purpose: The new lower eye lens dose limit is of relevance in interventional radiology, where higher dose procedures result in increased scattered radiation to staff. The eye lens dose may be monitored using the directional dose equivalent at 3 mm depth, $H_p(3)$, or through $H_p(10)$ or $H_p(0.07)$ measurements and using conversion factors. However, there are a considerable range of factors which contribute to measurement uncertainties, one of which is the incident photon energy. This study investigated the energy spectra of scattered radiation in interventional radiology, and the dosimetry accuracy of dosimeter types, evaluating their energy dependence.

Methods: Scatter X-ray energy spectra were recorded under varied conditions in a fluoroscopy imaging suite. Dosimetry accuracy of eye dosimeters, including TLDs (100 s, 100Hs), Landauer $H_p(3)$, John Caunt ED3 and Electronic Personal dosimeters (EPDs) were compared to air kerma measurements across a range of tube voltages.

Results: The variation of energy spectra with changing phantom thickness, spectrometer angulation and filtration are presented. The 100 and 100H TLDs, and EPDs showed a consistent air kerma response (within 10%) with changes in energy. The real-time silicon diode detectors showed a variable over response of between 10 and 25% across the energies investigated while Landauers dedicated $H_p(3)$ eye dosimeters showed considerable variation between dosimeters for similar conditions, a 17% variation at 50 kV_p.

Conclusion: The work aimed to validate the scattered energy spectra typically encountered in interventional radiology and to further determine the accuracy of eye dosimeters in relation to energy response variations.

1. Introduction/Lit review

The effect of ionising radiation on the eye lens has been the topic of many epidemiological studies [1–3]. The development of cataracts had previously been assumed to occur above a dose threshold of 0.5 Gy [4]; however, recent studies have shown the eye lens to have a much greater sensitivity than previously thought [1,5–7] and consequently, it has been recognised that the formation of cataracts can occur at doses lower than the original 0.5 Gy threshold. As a result, the most recently issued International Commission of Radiation Protection (ICRP) guidelines have recommended the reduction of eye dose limits from 150 mSv to 20 mSv per annum averaged over a five-year period with no more than 50 mSv received in one year [4,8]. The new limits have been enacted into legislation, in the form of the International Basic Safety Standards (BSS), with the new occupational dose limits taking effect on enactment [9].

The eye lens radiosensitivity has raised concerns particularly in areas of interventional radiology (IR) and cardiology (IC) [10] where physicians are in close proximity to the patient, the principal source of scattered X-ray radiation, and subsequently potentially subject to high scattered radiation doses. Prior to the recent ICRP guidance, it had been deemed sufficient to monitor the eye lens using either a dosimeter placed at the level of the thyroid or using the whole-body dosimeter measurement multiplied by a correction factor. This approximation proved reasonable where the limit was set at 150 mSv per annum [11]; however, during a review of these surrogate measurements in the context of the new guidance, and in preparation for the new legislation, it was found that many radiologists and cardiologist appeared to exceed the new dose limit [12]. As a result, there has been an increased focus on eye lens monitoring and radiation protection for staff members.

* Corresponding author.
E-mail address: maevemasterson95@gmail.com (M. Masterson).

https://doi.org/10.1016/j.ejmp.2019.11.002
Received 1 July 2019; Received in revised form 10 September 2019; Accepted 1 November 2019
Available online 07 November 2019

While the dose to the eye lens is not measured directly, dose metrics such as personal dose equivalents, $H_p(d)$, may be measured using dosimeters placed close to the organ of interest. Personal dose equivalent dosimeters measure the dose to a depth, d, in millimetres (mm) in tissue. The ICRP recommended the equivalent measurement depth of 3 mm ($H_p(3)$) for the eye lens [13,14]. As $H_p(3)$ dosimeters were limited at the time of the report, alternative techniques were investigated and developed. These have included the use of correction factors and applying them to detectors already in use, using available $H_p(0.07)$ detectors as a conservative measure and/or using conversion factors to convert between different operational quantities [8,11].

It has been highlighted that many factors may affect the dosimetry measurement uncertainty, including the type of scattering medium used within the dosimeter, whether a backscattering medium is employed during experiments, the X-ray beam geometry, the angle of incidence of the beam, the beam energy and range, and whether measurements are simulated or experimentally acquired [11]. Thorough investigations were carried out by ORAMED WP2 to establish a theoretical and experimental basis to assess eye lens doses [15]. The scope of their initial work involved investigating and developing a prototype for an $H_p(3)$ dosimeter (EYE-D^{TM}) meeting ISO and IEC performance standards. Included in these investigations were the performance of Thermoluminescence dosimeters (TLDs) Lif:Mg,Ti and LiF:Mg,Cu,P (TLD 100 and TLD 100H respectively) for their energy and angular response. The angular dependence of the EYE-D^{TM} prototype (LiF:Mg,Cu,P) fell within 20% for all obtained values between 0 and 80°. The relative energy response of Lif:Mg,Ti was shown to overestimate by 35% at 30 keV, whereas LiF:Mg,Cu,P displayed a characteristic minimum at 100 keV of 20% which was also observed in compared literature [15]. Indeed, when comparable tests were carried out in further studies, the energy response was identified as one of the most significant sources of error for eye dosimeters [15].

TLDs Lif:Mg,Ti and LiF:Mg,Cu,P and optically-stimulated luminescence dosimeters (OSLDs) have been seen to vary from unity depending on the incident photon energies. For example, it has been reported that a variation in OSLDs energy response of between 10 and 15% at 80 kV_p leads to an overestimation by 20% at a photon beam energy of 120 keV [16]. With regards to TLDs, the literature also suggests that both TLD types have a variable response at low X-ray energies, with the suggested deviations varying across studies [17]. Given that the typical scatter radiation energy range encountered for fluoroscopy procedures is reported to be in the 20–80 keV range [18,19] it is necessary to account for variations due to energy response to ensure dosimetric accuracy. Previous work towards evaluating the relative energy responses of dosimeters have done so against the selected peak tube voltage (kV_p); however, the primary X-ray beam in fluoroscopy is made up of a continuous spectrum of energies [20] and, furthermore, on interaction with a scattering medium, the resultant scattered energy spectrum is of a lower mean energy.

Accordingly, this study initially sought to measure and characterise the scattered X-ray energy spectra incident on staff under conditions and settings commonly encountered in interventional radiology. The accuracy of several detectors was evaluated and compared to air kerma for a range of clinically relevant scattered radiation energies. Air kerma measurements were used as a standard reference and obtained using a Radcal Ion camber. Furthermore, measured scatter energy spectral data was employed to estimate the relative energy response across the energy spectrum for each dosimeter type.

2. Materials and Methods

2.1. Characterising scatter energy spectra

A Siemens Axiom Artis DMP C-arm system (Siemens Healthcare, Erlangan Germany), was used to carry out the experimental aspect of this study. The peak tube voltage was varied across the range 50–81 kV_p, while the tube current was set in the 1–50 mA range. The X-ray tube was orientated in the under couch position, as would be typical for IR procedures, and 0.0–0.3 mm Cu filtration was employed. PMMA was used as a scattering medium with the centre of the PMMA positioned 97 cm from the tube focus and the focus to detector distance set at 120 cm.

The spectrometer used to characterise the scattered energy spectra was an Ortec Digidart-LF Portable MCA detector (Ametek-Ortec, PA, USA), consisting of a 1 × 1 in. 905 series Nal(Tl) scintillation detector, attached to a 2 in. photomultiplier tube (PMT), with a full width half maximum (FWHM) resolution of 8.1% for Cs-137 (661 keV). Maestro® multichannel analyses (MCA) software was used to analyse the spectra. To reduce the photon fluence and prevent saturation of the detector, low tube currents were used together with a 4 mm aperture lead pin-hole collimator placed over the crystal [21] in addition to a detector to PMMA distance adequate for ensuring the acceptance angle of the detector was large enough to receive the scattered photons from the PMMA. A single pin-hole aperture placed directly in front of the detector is the simplest form of collimation method and decreases the photon fluence by reducing the overall surface area of the detector [22]. To determine the effect of the pin-hole collimator on the spectra, scattered energy spectra were acquired with and without the collimator over a range of tube voltages, and a ratio of un-collimated to collimated counts for each energy channel was obtained as a correction factor for each peak tube voltage setting. Thereafter, spectra acquired with the pin-hole collimator in place were corrected for, normalised per mA and smoothed using a 5-point moving average across the energy channels. The linearity of the spectrometer with the collimator was measured using 20 cm of PMMA, the spectrometer was positioned at 0° (Fig. 1) and at a distance of 1 m from the centre of the phantom. Measurements were obtained for 50 kV_p, 60 kV_p, 70 kV_p and 80 kV_p with increasing tube currents acquired for a set time.

Scattered energy spectra were recorded for a range of experimental set ups. PMMA phantom thickness was varied between 10 and 25 cm (increments of 5 cm) to simulate differences in patient size, while the effect of changes in Cu filtration (0.0–0.3 mm Cu) and tube voltages on the scattered energy spectra were also investigated. For these investigations, the spectrometer was fixed at a distance of 1 m from the phantom centre and level with the centre of the phantom (0°). To examine the scatter at different angles from the phantom, the spectrometer was angled at 0°, 22.5° and 45° relative to the table (Fig. 1). The 45° angulation has previously been used for simulating scattered radiation to the eye [23]. Spectra were then recorded during live interventional radiology cases and compared to that obtained during the

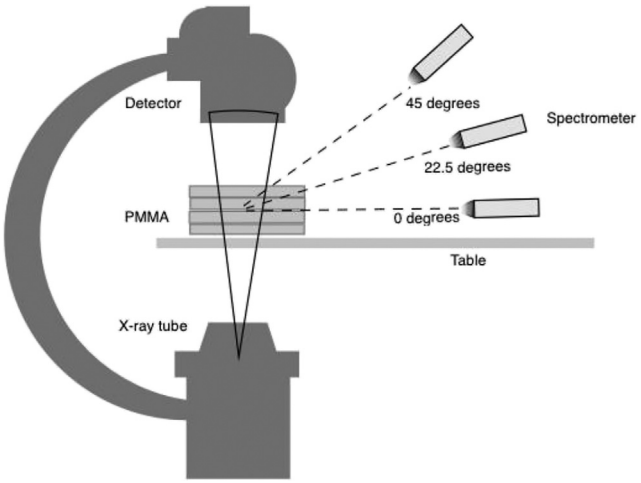

Fig. 1. Experimental set-up with spectrometer angulation investigations on the Siemens Axiom Artis DMP C-arm system with spectrometer positioned at 0, 22.5 and 45° and a set distance of 1 m from the centre of the PMMA.

previous preliminary experiments. The interventional radiology cases were carried out on using a Siemens Artis Q C-arm system (Siemens Healthcare, Erlangan Germany).

3. Evaluating detector response with energy

Five detectors types were studied in this work. These included TLD 100 s (LiF:Mg,Ti) and 100Hs (LiF:Mg,Cu,P), Thermo EPDs MK2+ (Thermo Fisher Scientific, MA, USA), John Caunt scientific (JCS) ltd (UK) real-time Hp(0.07) ED3 silicon diode detector and Landauer vision Eye dosimeters (Landauer, IL USA). The TLD 100 s and 100Hs were calibrated in house at 80 kV_p. TLDs were annealed prior to use and read 24 h after exposure using a Thermo Scientific^{TM} HARSHAW 5500 Automatic TLD Reader. EPDs were calibrated in-house against a ^{137}Cs reference source, exhibiting a measurement accuracy of ± 5%. The Landauer Vision $H_p(3)$ eye dosimeters were sent to Landauer to be read after experiments. The JCS D4 detectors, which are uncompensated detectors sensitive to energies in the range 33–60 keV were used to measure $H_p(0.07)$ with the ED3 detector system. Two D4 diodes were used and their correction factors, as suggested by the manufacturer, were employed. As the ED3 measures $H_p(0.07)$ it was necessary to employ a conversion coefficient to convert the quantity to air kerma. The accuracy and energy response of each dosimeter was compared against air kerma measured using a Radcal accu gold + system with 180 cc ion chamber (Radcal corporation, Ca, USA). The dosimeters were placed free in air, with no backscattering medium, alongside the ion chamber and spectrometer at a distance of 0.5 m from the centre of the scatter medium, 20 cm of PMMA, at a 0° orientation as per Fig. 1. It was ensured that all exposed dosimeters were positioned such that they were normal to the PMMA, to control for any angular dependence of the dosimeters themselves. The dosimeter responses were investigated for a range of tube voltages 50 kV_p, 55 kV_p, 60 kV_p, 63 kV_p, 66 kV_p, 70 kV_p, 73 kV_p, 77 kV_p and 81 kV_p exposed to an accumulated incident dose of approximately 200 μGy for each kV_p setting as recorded by Radcal system. For each tube voltage, a scattered energy spectrum was also recorded using the Ortec Digidart spectrometer.

The energy response of each detector was further investigated. To this end, the measured incident scatter energy spectrum for each kV_p setting was separated into 9 × 5 keV bins, from 31 to 76 keV, with the total count for each bin divided by the total counts for the entire spectrum. For each detector, determining the weighting of each 5 keV bin would offer information on the relative response of a detector to the incident photons of that energy bin. Thus, as each dosimeter type was exposed using 9 different energy spectra (50–81 kV_p), it was possible to solve for the weighting factors. This was solved numerically by employing the excel solver tool, a least squares fitting tool, which was used to calculate those weighting factors which minimise a Chi-squared goodness of fit function.

4. Results

When characterising the collimator using a scattered energy beam, it was shown that the spectrometer saturated at low tube currents, thus necessitating the application of the collimator. A collimator with a 4 mm pin-hole aperture was placed over the crystal to reduce the intensity of photons incident on the surface, preventing saturation. This reduced the effective surface area of the crystal from 5.07 cm^2 to 0.12 cm^2. Preliminary tests using a ^{99m}Tc point source showed a 98% reduction of the number of counts detected by the spectrometer. There were no evident effects on the spectra due to the addition of the lead collimator.

The response of the spectrometer with the collimator proved to be linear, with R-squared values of greater than 0.99 calculated for 50 kV_p, 70 kV_p and 80 kV_p and 0.98 for 60 kV_p. This is illustrated in Fig. 2 for a range of fluoroscopy tube currents exposed for a set time of 20 s. No detector saturation was evident for these ranges.

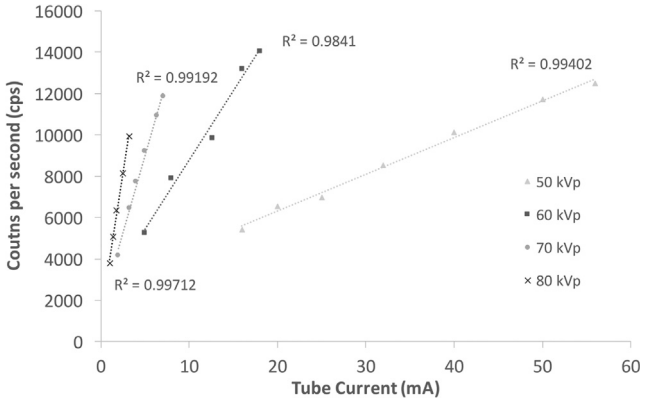

Fig. 2. Linearity of Ortec digi-dart spectrometer using a pin-hole collimator with fluoroscopy acquisitions acquired for a set time period of 20 s.

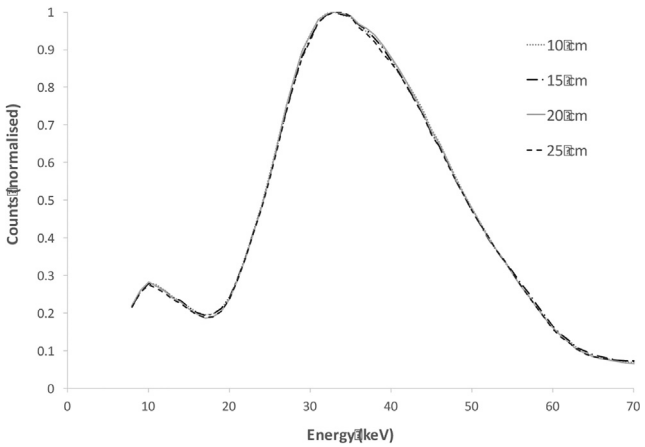

Fig. 3. Scattered energy spectra for varying phantom thickness (10–25 cm) at 70 kV_p.

The effect of patient thickness (10–25 cm) on the scattered energy spectra at a distance of 1 m and in line (at 0°) with the centre of the phantom was firstly investigated. This was carried out for peak tube voltage settings of 50 kV_p, 60 kV_p and 70 kV_p. Fig. 3 shows the collected energy spectra at a tube voltage of 60 kV_p for the varied thicknesses. While a variation in phantom thickness did impact the total counts for each spectrum (the intensity of the counts recorded reduced by 6% with an increase in phantom thickness from 10 cm to 25 cm), the spectra were normalised to the maximum spectral counts such that the energy spectrum profile could be examined. No significant variation between each of the collected spectra when normalised was observed for variations in thicknesses. This was also the case for the tube voltages of 50 and 70 kV_p, respectively.

The addition of copper filtration to the primary beam, which would be expected to lead to primary beam hardening, led to a spectral change of the scattered energy spectra. With no added filtration at 70 kV_p, the scattered energy spectra relative counts peaked at 34 keV, while the addition of 0.3 mm Cu caused this peak to increase to 44 keV (Fig. 4 (b)). Similarly, spectral hardening was also observed at lower peak tube voltages with the relative energy peak increasing from 31 keV and 33 keV to 34 keV and 39 keV for tube voltages of 50 and 60 kV_p, respectively. Fig. 4 (a) also illustrates how the addition of copper filtration reduced the overall intensity of the spectrum with the peak intensity of the 0.3 mm Cu spectrum being reduced by nearly 70% when compared to no filtration. The spectra in Fig. 4 (a) are normalised to the maximum value of the 0.0 mm Cu spectrum.

Scattered spectra resulting from the increase in detector angulation from 0° to 22.5° and 45° with the spectrometer maintained at a 1 m

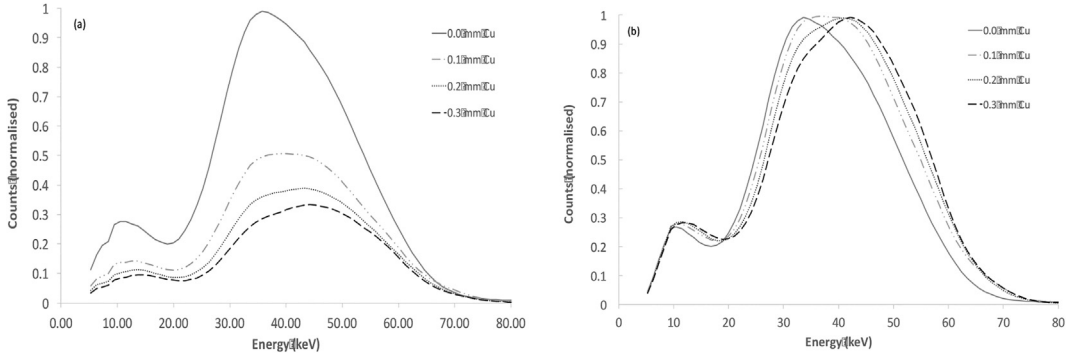

Fig. 4. Scatter energy spectra for added filtration, (a): normalised using the maximum counts obtained with no added filtration. (b): Scatter energy spectra normalised to maximum counts of each spectrum.

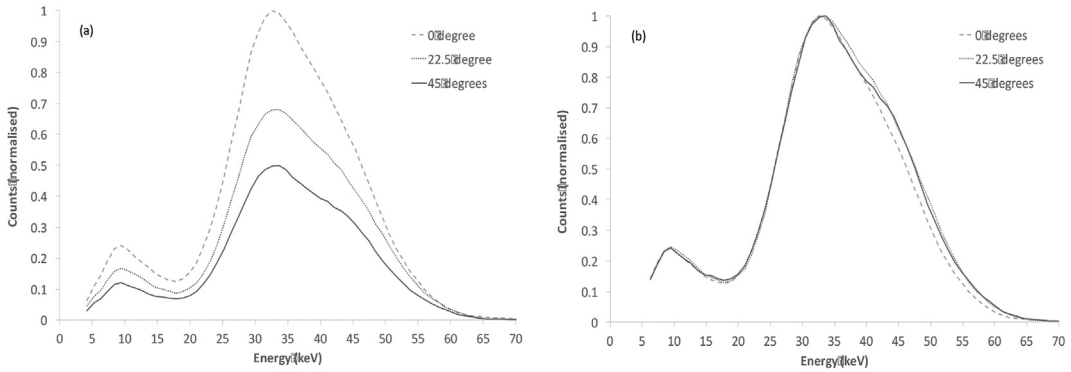

Fig. 5. Scatter energy spectra for varying spectrometer angle at a tube voltage of 60 kVp, (a): Spectra normalised to maximum counts obtained at 0°, (b): spectra normalised to maximum counts of each spectrum.

distance were examined with 20 cm of PMMA used as a scatter medium. It was noted that an increase in the angle led to a reduction in the number of counts recorded per mAs, by 32% and 50% for the 22.5° and 45° orientations, respectively (Fig. 5 (a)). Fig. 5 (b) is normalised to the maximum count from the 0° spectrum, it shows data of the three angulations at 60 kV_p, displaying the relative spectral counts to vary by approximately 10% between 30 and 40 keV and by 14% between 40 and 60 keV.

Energy spectra were measured during some live interventional radiology cases. Fig. 6 shows two embolism cases with a maximum tube voltage of 60 kV_p and 74 kV_p and compares with a controlled phantom study. 0.3 mm Cu filtration was used in each of the clinical studies and, for practical reasons, the spectrometer was placed at an angulation of 0° to the table at mid phantom height.

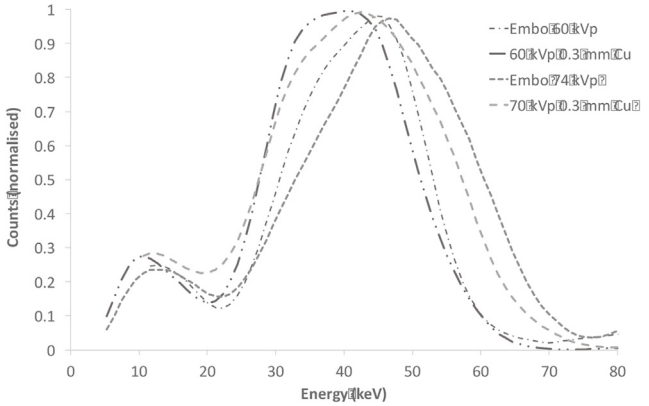

Fig. 6. Energy spectra for embolism collected during live interventional radiology cases plotted with data from the phantom study.

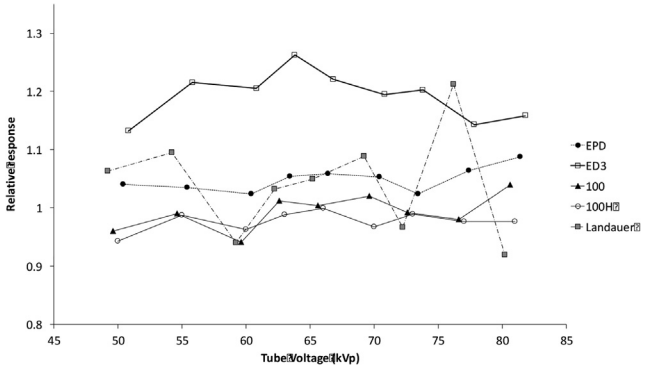

Fig. 7. Relative energy response of each dosimeter compared to air kerma.

Fig. 7 illustrates the relative energy response of each of the detectors when compared to the reference air kerma as measured using the Radcal 180 cc chamber, the average air kerma values for each dosimeter and reference air kerma are as displayed in Table 1. The relative energy response of TLD 100 s and 100Hs, agreed within 6% across all the peak tube voltages, EPDs showed an overestimation of between 2 and 9%. Using ISO monenergistic conversion coefficient [24], the ED3 dosimeter was converted from $H_p(0.07)$ to air kerma and was shown to overestimate the dose by between 10 and 25% depending on the tube voltage. Conversion factors based on G. Gualdrini et al. [25], was used to convert Landauer $H_p(3)$ dosimeters to air kerma. These showed a fluctuating relative response of 0.92 to 1.21 between 50 and 81 kV_p. Each point at each tube voltage represents the average of two measurements for each detector type with uncertainties based on the standard deviation of these two measurements. We have not investigated the intrinsic uncertainties of the different detectors but instead have considered the values as direct measures which would

Table 1
Energy response in Air Kerma (μGy) for each dosimeter. Measurements were recorded on two occasions, ED3, TLD 100H and TLD 100 are compared to air kerma (AK) Radcal (1) measurements. EPD and Landauer (Lan) $H_p(3)$ were compared to AK Radcal (2). Conversion coefficients were used to convert from $H_p(0.07)$ and $H_p(3)$ to air kerma for ED3 and Landauer $H_p(3)$.

Tube voltage (kVp)	AK Radcal (1) (μGy)	ED3 (μGy)	TLD 100H (μGy)	TLD 100 (μGy)	AK Radcal (2) (μGy)	EPD (μGy)	Lan $H_p(3)$ (μGy)
50	201.1	325.67	189.61	193.08	200.40	208.5	203.59
55	201.5	367.57	198.91	199.58	200.60	207.5	215.57
60	203.8	385.88	196.14	191.78	201.20	206	188.62
63	200.4	393.71	198.07	202.75	202.60	213.5	209.58
66	204.9	403.12	204.77	205.71	201.70	213.5	212.57
70	205.5	404.16	198.74	209.65	202.80	213.5	221.56
73	206.1	414.62	203.91	204.41	247.60	253.5	239.52
77	208.2	413.55	203.34	204.11	201.20	214	242.51
81	204.3	407.24	199.57	212.28	201.90	219.5	182.63

typically be the case in the clinical environment.

The relative energy response of each dosimeter was investigated to determine whether there was equal contribution to the dose across the energy spectrum. The relative energy response of each energy bin in the spectra was investigated for TLD 100 s, 100H, EPD and ED3 dosimeters. Landauer $H_p(3)$ dosimeters were excluded from this aspect of the study due to their large fluctuating response. ED3 dosimeter were shown to overestimate in the 45–50 keV energy bin with a maximum relative response of 1.81. TLD 100 s, 100Hs and EPDs were shown to have a contribution of within 6% across the energy spectrum (Fig. 8).

5. Discussion

In this work, we used a spectrometer to characterise the scattered energy spectra that would typically be encountered in an interventional radiology or fluoroscopy room and, further, investigated how some of the parameters that would be routinely varied clinically might affect the scattered spectra. This was of interest given that the literature has reported some dosimeter types to exhibit significant differences in their energy responses for the range of scattered photons encountered in interventional radiology [11,16]. However, there is limited detail in the literature [23,26,27] of such scattered spectra and, indeed, no data on how detectors used for eye dosimetry respond to such clinically relevant scattered spectra.

In order to measure the scattered energy spectra, it was first necessary to characterise the spectrometer used. The literature reports that detectors may be overly sensitive to photon fluence [22,26] or may not have sufficient energy resolution [26], with those suitable detectors often proving too large, cumbersome and expensive for purpose [21]. The sensitivity of a detector to photon fluence is affected by its pulse counting ability. To record two separate photons, there needs to be an adequate time delay between the two events to ensure either pulse pile-up does not occur or that the second event is counted and not missed [28]. Although yielding different results, pulse pile-up and dead-time are often not differentiated in the literature [28]; however, both are as a result of high photon flux incident on the detector and lead to count loss. The Ortec digidart spectrometer used in this work contains circuitry in the form of a pulse pile up rejecter with a threshold set to reject pulses that are detected as too close together by a fast channel analyser (500 ns) [29]. Although this circuitry will not eliminate pulse pile-up completely it was deemed sufficient for the purpose of this study and therefore no numerical corrections were applied for pulse pile, as has been previously been recommended [30].

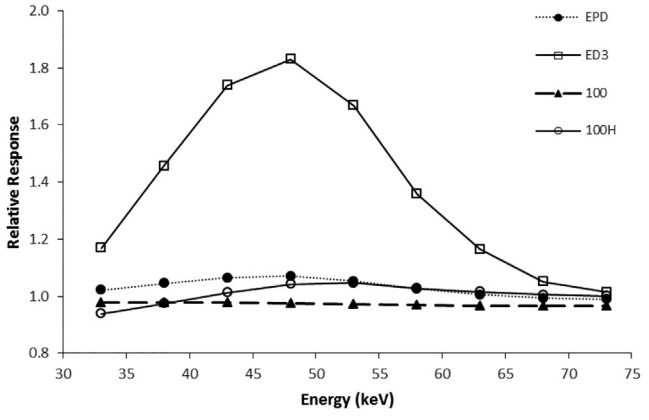

Fig. 8. Relative energy response per energy bin for EPDs, TLD 100 s, 100H and ED3 dosimeters.

The Ortec Digidart-LF detector employed was mobile, yet proved extremely sensitive and, hence, it was necessary to reduce the fluence incident on the detector using a pin-hole collimator. This has previously been explored in the literature with theoretical correction factors suggested, which use the crystal and collimator dimensions to account for the influence the collimator may have on the quantity of incident counts [22]; however, for the collimator and detector combination employed in this work the theoretical calculation did not represent the collimators influence on the spectra. The pin-hole collimator reduced the surface area of the detector from 5.07 cm^2 to 0.12 cm^2, reducing the overall intensity by as much as 98% from a point source of ^{99m}Tc, in line with the reduction in the effective crystal size for a relatively monoenergetic source. The lead collimator was sufficient to shield the crystal at the lower energy range used in interventional radiology, however, as the energy of the photons increases so does the penetration, therefore changing the efficiency of the collimator [22]. It was thus necessary to acquire energy spectra with and without the pin-hole collimator attached to the detector for each kV_p, to account for the varying conditions and the pin-hole effect. The detector response proved to be linear, deeming the spectrometer to be suitable for our purposes.

The collected scattered energy spectra gave useful information with regards the energy range of interest in interventional radiology. The intensity (counts) of the scattered spectra per mAs was shown to reduce by 6% with the increase in phantom thickness from 10 cm to 25 cm, without any significant change in the relative spectrum profile. In the clinical setting, automatic exposure control (AEC) would compensate for the size differences between patients, adjusting the tube voltage and current in order to maintain image quality [20]. The results show the mean energy of the scattered spectra to be between 33 and 35 keV for tube voltages of 50–70 kV_p, varying phantom thickness and spectrometer angulation. Further, the spectra gathered demonstrated how the presence of copper filtration in the primary X-ray beam affected the greatest influence on the scattered energy spectra manifesting as spectral hardening. Comparing the scattered energy spectra to the primary beam spectra was not possible in this work due to the sensitivity of the spectrometer to photon fluence; however, Monte Carlo simulations to compare primary and scattered spectra for a 70 kV_p X-ray beam and copper filtration have shown the scattered spectrum to exhibit a lower mean energy when compared to the primary spectrum [27]. These simulated results corroborate with the experimental work presented in this study. Indeed, this is of interest given that dosimeters and detectors used in diagnostic radiology are typically calibrated using primary X-ray beams of higher kV_ps and with higher mean energies than those used clinically [31]. Finally, preliminary measurements were recorded during live interventional radiology cases on a different system to the experimental measurements. We have not directly compared the two sets of data as the experimental data was measured in a controlled environment while the live cases were measured in a live working clinical environment. The purpose of this piece was to demonstrate that it was feasible to measure the scattered spectra in the

clinical environment; however, a more in depth examination of this topic is prompted for future work.

The energy responses of the detectors used in this work were investigated within the typical diagnostic X-ray energy range. The reliability of dosimeters in interventional radiology is of significance in order to accurately measure the dose received by staff in close proximity to the patient. The angular response of the detectors was not investigated in this study and was controlled for by maintaining an incident angle of 0°. Contrary to the literature [15,17], our results showed the energy response of the TLDs to have little dependence on the incident energy, with the relative energy response within 6% of the air kerma measurements. When investigated for energy dependence across the entire spectrum, for 5 keV energy bins, both TLD types were calculated to measure within 5% of the air kerma measurement. Accordingly, the TLD 100 s and 100 Hs proved to be ideal for eye dosimetry, provided an appropriate conversion factor to $H_p(3)$ is selected. Similarly, the EPDs which are typically used to measure whole body doses showed a consistent energy response of between 1.02 and 1.08 within the measured energy range, albeit these dosimeters are bulky and, therefore, would not practical for use in measuring eye doses in the clinical environment. In contrast, the ED3 dosimeters which are typical for $H_p(0.07)$ measurement were shown to overestimate air kerma by 10 to 25%. Again, the energy dependence of the detector was assessed per 5 keV energy bin with a less consistent response evident (Fig. 8). The highest relative response was in the 46–50 keV energy range, coinciding with the 50 keV peak response as stated by the manufacturers. The advantages of the ED3 dosimeters lie with their subtle size and real-time monitoring capabilities. In accounting for the ED3 energy dependence and subsequently improving the accuracy of the dosimeter, the detector could prove to be a very useful tool. The relative response of the Landauer Vision $H_p(3)$ detector was shown to deviate from the air kerma measurement by as much as 21% at 77 kV_p, where we assumed an air kerma to $H_p(3)$ factor of 1.66 for this energy based on factors published by Gualdrini et al. [25]. Knowledge of the exact conversion factor used by the company was not known. The energy response of the EYE-D™ prototype showed an energy response of within 10% [11]. The results of this study lie within ISO performance standards which have an energy response criterion of ± 50% and within ORAMED WP2 recommended range of ± 30% [15]. However, taking into account the work load and energy range used in Interventional Radiology and Cardiology, the over-response of ED3 and Landauer $H_p(3)$ detectors could lead to overestimates. While the other dosimeters displayed predictable trends, respectively, of changes in response with energy, this was not the case with the Landauer dosimeters. Indeed, in addition, the standard deviations of the $H_p(3)$ detectors were notably high in comparison to the other dosimeters with a maximum coefficient of variation (CV) of 17% at 50 kV_p, ISO recommend a CV of within 10% [15]. This was most prominent at 50 kV_p where relative responses of 0.94 and 1.19 were recorded for the dosimeters employed. This large CV meant it was not possible to determine the contribution of each 5 keV energy bin to the overall energy response. In this work only 2 dosimeters were used for each set kV_p measurement and, thus, further work on the agreement and accuracy of the Landauer $H_p(3)$ Vision dosimeters is merited.

This study focused on the relative response of dosimeters to air kerma and presents a methodology for such evaluation; however, it is necessary to use conversion factors to convert to $H_p(3)$ data in order to account for the dose to the eye lens. A number of such factors and operational quantities have been published in the literature from both independent research groups and from recognised international organisations, such as the ICRU and ICRP [11]. There appear to be variations in the methodology as to how these values are obtained and there are also differences in the published air kerma to $H_p(3)$ conversion coefficients [7,9,27]. Thus, while in this work every effort has been made to investigate and account for the energy responses of dosimeters used for monitoring of the eye lens, the resultant estimated dose from an exposure could be significantly different depending on the $H_p(3)$ conversion coefficients used. On a practical level, this could lead to an overestimation of eye lens dose and, thus, a potentially unnecessary curtailing of workload for staff members who may be approaching and/or exceeding the eye lens limits of the latest legislation. On the contrary, an underestimation may unknowingly put staff at risk of receiving a higher eye lens dose than the legal limit [11]. Therefore, there is a clear need for the factors affecting dosimeter accuracy to be established and accounted for, and also for there to be international agreement on $H_p(3)$ conversion coefficients.

6. Conclusion

In this study we present a means of investigating the relative response of dosimeters to incident energy. Unshielded scattered energy spectra typically encountered in interventional radiology or fluoroscopy suites have been presented and some investigations as to the parameters which affect these spectra have been reported. A range of different dosimeter types were investigated for their energy dependence as compared with air kerma measurements. We report 100 and 100H TLDs, and those EPDs evaluated in this work, to show a consistent response to changes in energy, as compared with air kerma. The real-time silicon diode detectors showed a variable response across the energies investigated while Landauers dedicated $H_p(3)$ eye dosimeters were shown to exhibit considerable variation across dosimeters for similar conditions. Indeed, while the focus of this work has been to improve the accuracy of eye dosimeters by accounting for energy response variations, the ultimate estimated eye dose accuracy may be further subject to the $H_p(3)$ conversion factors used.

Acknowledgements

We would like to acknowledge the Institute of Physics and Engineering in Medicine (IPEM) for supplying the Research and Innovation grant to purchase the spectrometer used in this study. Further, to thank National College of Ireland, Galway, where this study was undertaken as part of a postgraduate project.

References

[1] Chodick G, Bekiroglu N, Hauptmann M, Alexander BH, Freedman DM, Doody MM, et al. Risk of cataract after exposure to low doses of ionizing radiation: a 20-year prospective cohort study among US radiologic technologists. Am. J. Epidemiol. 2008;168:620–31. https://doi.org/10.1093/aje/kwn171.

[2] Kleiman NJ. Radiation cataract. Ann. ICRP. 2012;41:80–97. https://doi.org/10.1016/j.icrp.2012.06.018.

[3] Bitarafan Rajabi A, Noohi F, Hashemi H, Haghjoo M, Miraftab M, Yaghoobi N, Rastgou F, Malek H, Faghihi H, Firouzabadi H, Asgari S, Rezvan F, Khosravi H, Soroush S, Khabazkhoob M. Ionizing radiation-induced cataract in interventional cardiology staff. Res. Cardiovasc. Med. 2015;4:e25148. https://doi.org/10.5812/cardiovascmed.25148.

[4] ICRP, ICRP Statement on Tissue Reactions/ Early and Late Effects of Radiation in Normal Tissues and Organs - Threshold Doses for Tissue Reactions in a Radiation Protection Context. ICRP Publication 118. Ann. ICRP 41(1/2), (2012).

[5] Ciraj-Bjelac O, Rehani MM, Sim KH, Liew HB, Vano E, Kleiman NJ. Risk for radiation-induced cataract for staff in interventional cardiology: Is there reason for concern? Catheter. Cardiovasc. Interv. 2010;76:826–34. https://doi.org/10.1002/ccd.22670.

[6] Rehani MM, Vano E, Ciraj-Bjelac O, Kleiman NJ. Radiation and cataract. Radiat. Prot. Dosimetry. 2011;147:300–4. https://doi.org/10.1093/rpd/ncr299.

[7] Vano E, Gonzalez L, Fernández JM, Haskal ZJ. Eye lens exposure to radiation in interventional suites: caution is warranted. Radiology 2008;248:945–53. https://doi.org/10.1148/radiol.2482071800.

[8] Behrens R, Dietze G. Monitoring the eye lens: which dose quantity is adequate? Phys. Med. Biol. 2010;55:4047–62. https://doi.org/10.1088/0031-9155/55/14/007.

[9] IAEA, Radiation Protection and Safety of Radiation Sources: International Basic Safety Standards, IAEA Safety Requirements Part 3, (2014). https://www.iaea.org/publications/8930/radiation-protection-and-safety-of-radiation-sources-international-basic-safety-standards (accessed September 10, 2019).

[10] Nowak M, Sans-Merce M, Lemesre C, Elmiger R, Damet J. Eye lens monitoring programme for medical staff involved in fluoroscopy guided interventional procedures in Switzerland. Phys. Medica Eur. J. Med. Phys. 2019;57:33–40. https://doi.

org/10.1016/j.ejmp.2018.12.001.
[11] Carinou E, Ferrari P, Bjelac OC, Gingaume M, Merce MS, O'Connor U, et al. review. J. Radiol. Prot. 2015;35(2015):R17–34. https://doi.org/10.1088/0952-4746/35/3/R17.
[12] Martin CJ, Magee JS. Assessment of eye and body dose for interventional radiologists, cardiologists, and other interventional staff. J. Radiol. Prot. 2013;33:445. https://doi.org/10.1088/0952-4746/33/2/445.
[13] ICRU, Report 57, J. Int. Comm. Radiat. Units Meas. os29 (1998) NP-NP. doi:10.1093/jicru/os29.2.Report57.
[14] ICRP, ICRP Publication 103: The 2007 Recommendations of the International Commission on Radiological Protection, (2007). http://www.icrp.org/publication.asp?id=ICRP%20Publication%20103 (accessed August 18, 2019).
[15] Vanhavere F, Carinou E, Gualdrini G, Clairand I, Merce MS, Ginjaume M. The ORAMED Project: Optimisation of Radiation Protection for Medical Staff. In: Dössel O, Schlegel WC, editors. World Congr. Med. Phys. Biomed. Eng. Sept. 7–12 2009 Munich Ger. Springer Berlin Heidelberg; 2009. p. 470–3.
[16] Al-Senan RM, Hatab MR. Characteristics of an OSLD in the diagnostic energy range. Med. Phys. 2011;38:4396–405. https://doi.org/10.1118/1.3602456.
[17] Koukorava C, Farah J, Struelens L, Clairand I, Donadille L, Vanhavere F, et al. Efficiency of radiation protection equipment in interventional radiology: a systematic Monte Carlo study of eye lens and whole body doses. J. Radiol. Prot. 2014;34:509. https://doi.org/10.1088/0952-4746/34/3/509.
[18] Chiriotti S, Ginjaume M, Vano E, Sanchez RM, Fernandez JM, Duch MA, et al. Performance of several active personal dosemeters in interventional radiology and cardiology. Radiat. Meas. 2011;46:1266–70. https://doi.org/10.1016/j.radmeas.2011.05.073.
[19] Mitchell EL, Furey P. Prevention of radiation injury from medical imaging. J. Vasc. Surg. 2011;53:22S–7S. https://doi.org/10.1016/j.jvs.2010.05.139.
[20] Bushberg JT, Seibert JA, Leidholdt EM, Boone JM. The Essential Physics of Medical Imaging. Third: Lippincott Williams and Wilkins; 2012.
[21] Maeda K, Matsumoto M, Taniguchi A. Compton-scattering measurement of diagnostic X-ray spectrum using high-resolution Schottky CdTe detector. Med. Phys. 2005;32:1542–7. https://doi.org/10.1118/1.1921647.
[22] Kodera Y, Chan H-P, Doi K. Effect of collimators on the measurement of diagnostic X-ray spectra. Phys. Med. Biol. 1983;28:841–52. https://doi.org/10.1088/0031-9155/28/7/006.
[23] Marshall NW, Faulkner K, Warren H. Measured scattered X-ray energy spectra for simulated irradiation geometries in diagnostic radiology. Med. Phys. 1996;23:1271–6. https://doi.org/10.1118/1.597690.
[24] Kharrati H, Zarrad B. Computation of conversion coefficients relating air Kerma to Hp(0.07, α), Hp(10, α), and for X-ray narrow spectrum from 40 to 140 kV. Med. Phys. 2004. https://doi.org/10.1118/1.1637968.
[25] Gualdrini G, Bordy JM, Daures J, Fantuzzi E, Ferrari P, Mariotti F, et al. Air kerma to HP(3) conversion coefficients for photons from 10 keV to 10 MeV, calculated in a cylindrical phantom. Radiat. Prot. Dosimetry. 2013;154:517–21. https://doi.org/10.1093/rpd/ncs269.
[26] Dick CE, Soares CG, Motz JW. X-ray scatter data for diagnostic radiology. Phys. Med. Biol. 1978;23:1076–85. https://doi.org/10.1088/0031-9155/23/6/003.
[27] Zagorska A, Bliznakova K, Buchakliev Z. Towards the estimation of the scattered energy spectra reaching the head of the medical staff during interventional radiology: A Monte Carlo simulation study. J. Phys. Conf. Ser. 2015;637:12036. https://doi.org/10.1088/1742-6596/637/1/012036.
[28] Usman S, Patil A. Radiation detector deadtime and pile up: A review of the status of science. Nucl. Eng. Technol. 2018;50:1006–16. https://doi.org/10.1016/j.net.2018.06.014.
[29] Ortec, digiDART High Performance Portable Digital MCA | Multichannel Analyzer | AMETEK ORTEC, (2010). https://www.ortec-online.com/products/electronics/multichannel-analyzers-mca/portable/digidart (accessed June 19, 2019).
[30] Cano-Ott D, Tain JL, Gadea A, Rubio B, Batist L, Karny M, et al. Pulse pileup correction of large NaI(Tl) total absorption spectra using the true pulse shape. Nucl. Instrum. Methods Phys. Res. Sect. Accel. Spectrometers Detect. Assoc. Equip. 1999;430:488–97. https://doi.org/10.1016/S0168-9002(99)00216-8.
[31] Bordy JM, Daures J, Denozière M, Gualdrini G, Ginjaume M, Carinou E, et al. Proposals for the type tests criteria and calibration conditions of passive eye lens dosemeters to be used in interventional cardiology and radiology workplaces. Radiat. Meas. 2011;46:1235–8. https://doi.org/10.1016/j.radmeas.2011.07.035.